22

Wind Energy Conversion

Dale E. Berg
*Sandia National Laboratories**

22.1 Introduction

Wind energy is the most rapidly expanding source of energy in the world today. Over the past 10 years, the worldwide installed capacity of wind energy has grown at an average rate of over 28% per year, leading to an installed nameplate capacity at the end of 2004 of about 48,000 MW, enough to power about 16 million average American homes. As of January 2005, Germany was the world leader in wind-energy installations with about 16,600 MW installed, followed by Spain with 8300, the US with 6700, Denmark with 3100, India with 3000, Italy with 1100, The Netherlands with 1100, the United Kingdom with 900, Japan with 900, and China with 800. Although wind power supplies only about 0.6% of the world electricity demand today, the size of that contribution is growing rapidly. In Germany, the contribution of wind power to electricity consumption is over 5%, in Spain it is about 8%, and in Denmark it is approximately 20%. The cost to generate wind energy has decreased dramatically from more than 30 cents (U.S.) per kilowatt-hour (¢/kWh) in the early 1980s to under 4¢/kWh (at the best sites) in 2004. The cost has actually increased somewhat in the recent past, in spite of continuing technological improvements, as a result of worldwide increases in steel, concrete, and transportation

*Sandia is a multiprogram laboratory operated by Sandia Corporation, a Lockheed Martin Company, for the United States Department of Energy's National Nuclear Security Administration under contract DE-AC04-94AL85000.

costs that have led to increases in the prices of wind turbines. The large increases in the cost of natural gas and other fossil fuels have made wind-generated electricity a lower-cost option than natural gas for many utilities adding generating capacity. In fact, the demand for wind energy in the United States has been so strong that wind-power developers are demanding and receiving significantly higher prices in their new long-term power purchase agreements with utility companies than they did 2 years ago.

There is considerable anecdotal evidence that the first wind machines may have been built over 2000 years ago, perhaps in China, but there is no firm evidence to support this conjecture. However, there is considerable written evidence that the windmill was in use in Persia by AD 900, and, perhaps, as early as AD 640. Figure 22.1 illustrates the main features of this type of mill. The center vertical shaft was attached to a millstone and horizontal beams or arms were attached to the shaft above the millstone. Bundles of reeds attached vertically to the outer end of the arms acted as sails, turning the shaft when the wind blew. The surrounding structure was oriented so that the prevailing wind entered the open portion of the structure and pushed the sails downwind. The closed portion of the structure sheltered the sails from the wind on the upwind pass. The primary applications of these machines were to grind or mill grain and to pump water; they became generally known as *windmills*. The wind turbines of today may look much different than those first machines, but the basic idea remains the same—use the power in the wind to generate useful energy. Modern wind machines, called *wind turbines*, tend to have a small number of airfoil-shaped blades, in contrast to the older windmills that usually had several flat or slightly curved blades (such as the American multiblade water pumper shown in Figure 22.2). The reasons for this difference in blade number will be examined later in this chapter.

Although there are many different configurations of wind turbines, most of them can be classified as either horizontal-axis wind turbines (HAWTs), which have blades that rotate about a horizontal axis parallel to the wind, or vertical-axis wind turbines (VAWTs), which have blades that rotate about a vertical axis. Figure 22.3 illustrates the main features of these configurations. They both contain the same major components, but the details of those components differ significantly.

According to Shepard [1], the terms "horizontal" and "vertical" associated with these classifications are a potential source of confusion. Although they now refer to the driving shaft on which the rotor is mounted, in the past these terms referred to the plane in which the rotor turned. Thus, the ubiquitous multibladed water-pumper windmill shown in Figure 22.2, now referred to as a *horizontal-axis machine*,

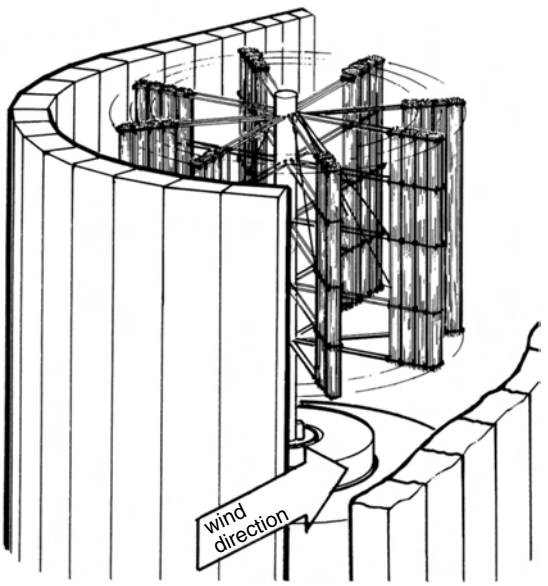

FIGURE 22.1 Illustration of ancient Persian wind mill.

FIGURE 22.2 Typical American multiblade windmill. (Courtesy of Nolan Clark, U.S. Department of Agriculture).

had a rotor that turned in a vertical plane, and was therefore at one point known as a *vertical* mill. Likewise, the earliest windmills, such as the one illustrated in Figure 22.1, had rotors that turned in a horizontal plane, and were known as *horizontal* windmills.

As shown in Figure 22.3, HAWTs and VAWTs have very different configurations. Each configuration has its own set of strengths and weaknesses. HAWTs usually have all of their drive train (the transmission, generator, and any shaft brake) equipment located in a nacelle or enclosure mounted on a tower, as shown. Their blades are subjected to cyclic stresses due to gravity as they rotate, and their rotors must be oriented (yawed) so the blades are properly aligned with respect to the wind. HAWTs may be readily placed on tall towers to access the stronger winds typically found at greater heights. The most common type of modern HAWT is the propeller-type machine, and these machines are generally classified according to the rotor orientation (upwind or downwind of the tower), blade attachment to the main shaft (rigid or hinged), maximum power control method (full or partial-span blade pitch or blade stall), and number of blades (generally two or three blades).

VAWTs, on the other hand, usually have most of their drive train on the ground; their blades do not experience cyclic gravitational stresses and do not require orientation with respect to the wind. However, VAWT blades are subject to severe alternating aerodynamic loading due to rotation, and VAWTs cannot readily be placed on tall towers to exploit the stronger winds at greater heights. The most common types of modern VAWTs are the Darrieus turbines, with curved, fixed-pitch blades, and the "H" or "box" turbines with straight fixed-pitch blades. All of these turbines rely on blade stall (loss of lift and increase in drag as the blade angle of attack increases) for maximum power control. Although there are still a few manufacturers of VAWTs, the overwhelming majority of wind turbine manufacturers devote their efforts to developing better (and usually larger) HAWTs.

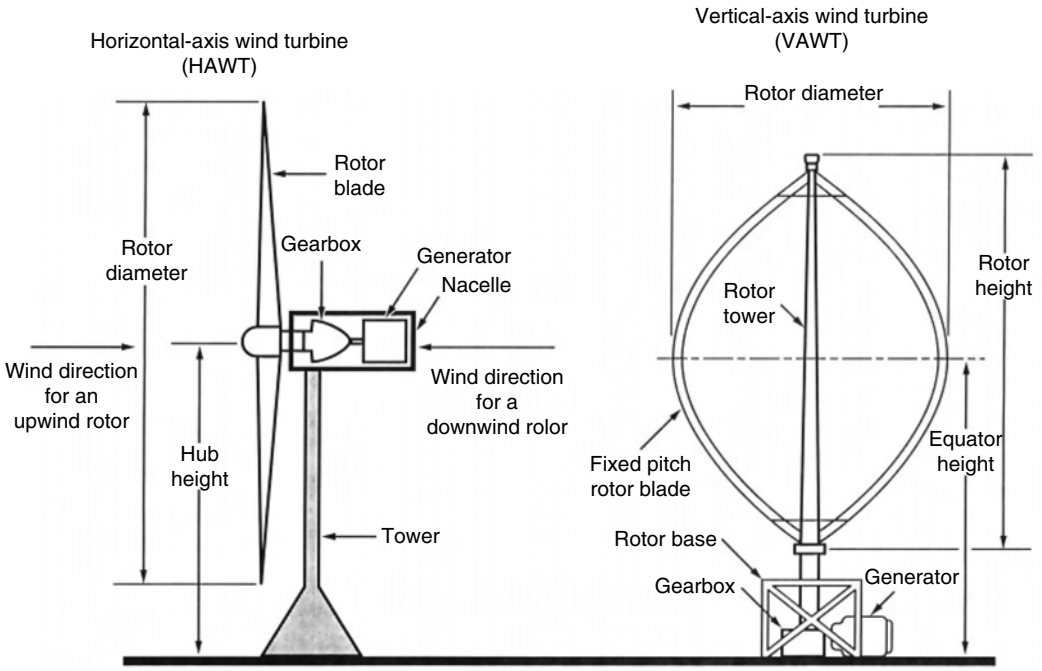

FIGURE 22.3 Schematic of basic wind turbine configurations.

Although the fuel for wind turbines is free, the initial cost of a wind turbine is a very large contributor to the cost of energy (COE) for that turbine. To minimize that COE, wind turbine designs must be optimized for the particular site or wind environment in which they will operate. Trial and error methods become very expensive and time-consuming when used to design and/or optimize turbines, especially larger ones. A large optimized wind turbine can be developed at a reasonable cost only if the designers can accurately predict the performance of conceptual machines and use modeling to investigate the effects of design alternatives. Over the past two decades, numerous techniques have been developed to accurately predict the aerodynamic and structural dynamic performance of wind turbines. These analytical models are not, in general, amenable to simple approximations, but must be solved with the use of computer codes of varying complexity. Several of these models are summarized below.

22.2 Wind Turbine Aerodynamics

Items exposed to the wind are subjected to forces in both the drag direction (parallel to the air flow) and the lift direction (perpendicular to the air flow). The earliest wind machines, known as *windmills*, used the drag on the blades to produce power, but many windmill designs over the last few centuries have made limited use of lift to increase their performance. For predominantly drag machines, such as those illustrated in Figure 22.1 and Figure 22.2, larger numbers of blades result in higher drag and produce more power; therefore, these machines tend to have many blades. The old Dutch windmills, such as the one shown in Figure 22.4, utilized lift as well as drag, and because lift devices must be widely separated to generate the maximum possible amount of power, those machines evolved with a small number of blades. The high-lift, low-drag shapes, referred to as *airfoils*, that were developed for airplane wings and propellers in the early part of the twentieth century were quickly incorporated into wind machines to produce the first modern wind machines, usually known as *wind turbines*. An example of a typical modern wind turbine is shown in Figure 22.5. Wind turbines use the lift generated by the blades to produce power. Because the blades must be widely separated to generate the maximum amount of lift,

FIGURE 22.4 Example of Dutch windmill. (Courtesy of Richard A. Neiser, Jr.).

lift-type machines have a small number of blades. The following paragraphs contrast the characteristics of the drag-type and lift-type machines.

Figure 22.6 illustrates the flow field about a moving drag device. The drag results from the relative velocity between the wind and the device, and the power that is generated by the device (the product of the drag force and the translation or blade velocity) may be expressed as

$$P = Dlv = [1/2\rho(U - v)^2]C_D clv, \tag{22.1}$$

where P is the power extracted from the wind, D is the drag force per unit length in the span direction (into the page), l is the length of device in the span direction (into the page), v is the translation (or blade) velocity, ρ is the air density, U is the steady free-stream wind velocity, $C_D = \text{Drag}/(1/2pclU^2)$ (drag coefficient, a function of device geometry), and c is the device width (perpendicular to the wind, in the plane of the page).

The translation (or blade) velocity of the device must always be less than the wind velocity or no drag is generated and no power is produced. The power extraction efficiency of the device may be expressed as the ratio of the power extracted by the device to the power available in the wind passing through the area occupied by the device (the projected area of the device), a ratio known as the *power coefficient*, C_p. From Equation 18.7, the power available is

$$P_A = \frac{1}{2}\rho U^3 A = \frac{1}{2}\rho U^3 cl,$$

where A is the area of the device projected perpendicular to the wind (cl).

Using Equation 22.1, the C_p for a drag machine is

$$C_P = \frac{P}{1/2\rho U^3 cl} = \frac{v}{U}\left[1 - \frac{v}{U}\right]^2 C_D. \tag{22.2}$$

FIGURE 22.5 General Electric 1.5-MW wind turbines near Lamar, Colorado.

Now consider a device that utilizes lift to extract power from the wind, i.e., an airfoil. Figure 22.7 depicts an airfoil that is moving at some angle relative to the wind and is subject to both lift and drag forces. The relative wind across the airfoil is the vector sum of the wind velocity, U, and the blade velocity, v. The angle between the direction of the relative wind and the airfoil chord (the straight line from the leading edge to the trailing edge of the airfoil) is termed the angle of attack, α. The power extracted by this device may be expressed as

$$P = 1/2\rho U^3 cl \frac{v}{U}\left[C_L - C_D \frac{v}{U}\right]\sqrt{1 + \left(\frac{v}{U}\right)^2}, \tag{22.3}$$

where c is the chord length, and

$$C_L = \frac{\text{Lift}}{1/2\rho clU^2} (\text{where lift is the coefficient, a function of airfoil shape and } \alpha),$$

$$C_D = \frac{\text{Drag}}{1/2\rho clU^2} (\text{where drag is the coefficient, a function of airfoil shape and } \alpha).$$

The other quantities are as defined for Equation 22.1. Lift and drag coefficients for some common airfoils may be found in the literature [2–7]. In this case, the projected area of the device is cl, and the power

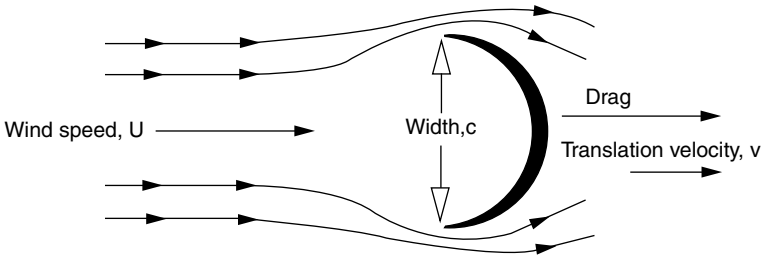

FIGURE 22.6 Schematic of translating drag device.

coefficient, using Equation 22.3, is

$$C_P = \frac{\nu}{U}\left[C_L - C_D\frac{\nu}{U}\right]\sqrt{1+\left(\frac{\nu}{U}\right)^2}. \tag{22.4}$$

Keep in mind that Equation 22.2 and Equation 22.4 express the performance coefficients of these devices in terms of the projected area of the individual device. Figure 22.8 presents experimental lift and drag coefficient values for the S-809 airfoil designed by the National Renewable Energy Laboratory (NREL) for use on small HAWTs [8]. As the angle of attack increases beyond approximately 9°, the lift levels off and then drops slightly and the drag begins to rise rapidly. This is due to separation of the flow from the upper surface of the airfoil, a flow condition referred to as *stall*. Figure 22.9 compares Equation 22.2 and Equation 22.4 using $C_L = 10$ and $C_D = 0.10$ for the airfoil (conservative values for modern airfoils, as seen from Figure 22.8), and a drag coefficient of 2.0 (the maximum possible) for the drag device. The airfoil has a maximum power coefficient of about 15, compared with 0.3 for the drag device, i.e., it extracts 50 times more power per unit of device surface area. Of course, the airfoil must be translated across the wind to produce power, but this is easily achieved with rotating machines such as wind turbines.

As mentioned earlier, lift-type machines tend to have only a few blades, while drag-type machines tend to have many blades. Thus, the difference in the turbine performance coefficient (now based on the rotor

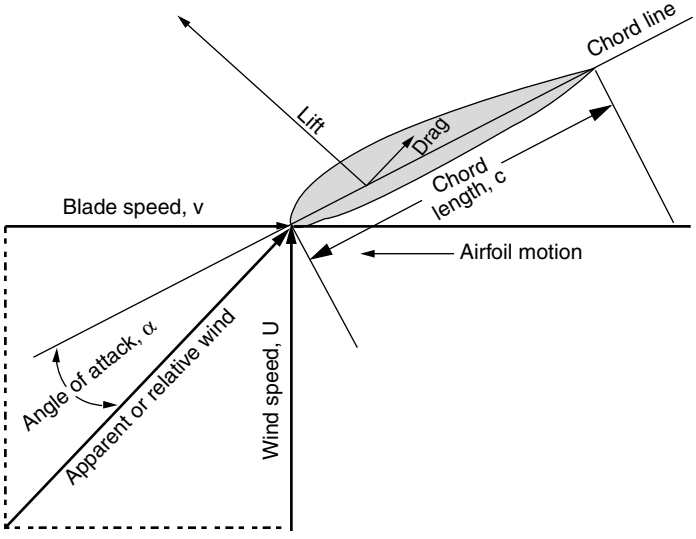

FIGURE 22.7 Schematic of translating lift device.

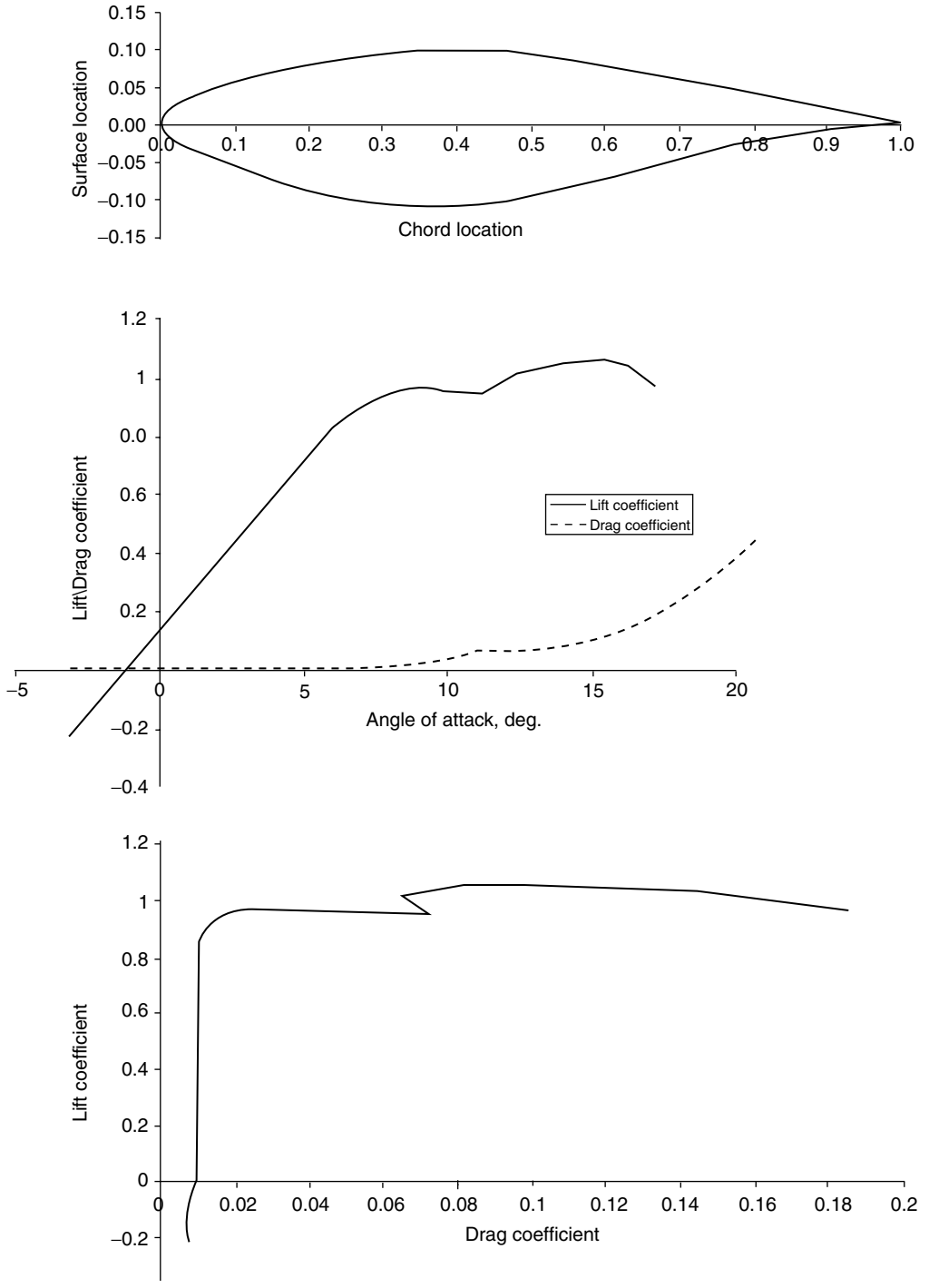

FIGURE 22.8 Profile and performance characteristics of the S-809 airfoil.

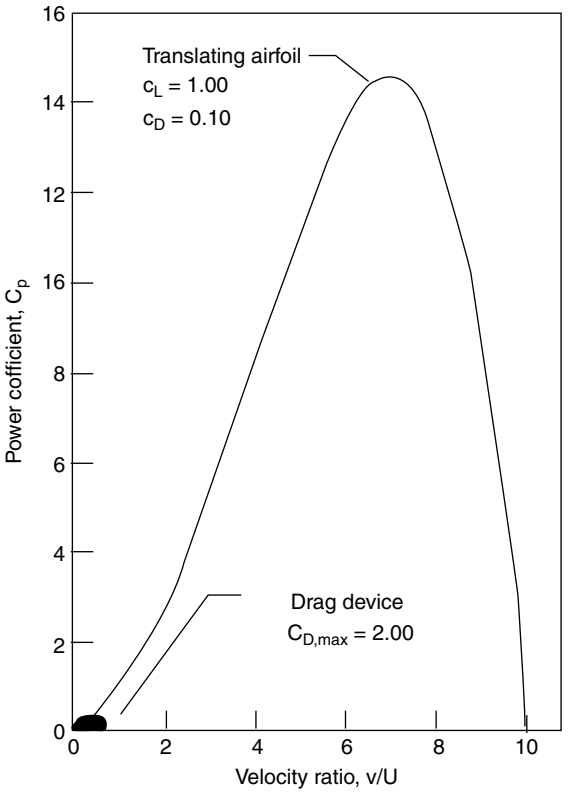

FIGURE 22.9 Comparison of power coefficients for drag-type and lift-type devices.

frontal area rather than the blade or bucket frontal area) of actual wind machines is much less than might be expected from the analysis presented above. A well-designed lift-type machine may achieve a peak power coefficient (based on the area covered by the rotating turbine blades) of 0.5–0.59, while a pure drag-type machine may achieve a peak power coefficient of no more than 0.2. Some of the multibladed drag-type windmills actually utilize a blade shape that creates some lift, and they may achieve power coefficients of 0.3 or slightly higher. The drag machines rotate slowly (the blade translation velocity cannot exceed the effective windspeed) and produce high torque, whereas the lift machines rotate quickly (to achieve a high translation velocity) and produce low torque. The slow-rotating, high-torque drag machines are very well-suited for mechanical power applications such as milling grain and pumping water. On the other hand, extensive experience has shown that fast-rotating, lift-type machines are much easier to adapt to electrical generators and can produce electricity at a significantly lower COE than drag-type machines. Because of their superior performance, only lift-type machines will be considered in the remainder of this chapter.

22.2.1 Aerodynamic Models

The aerodynamic analysis of a wind turbine has two primary objectives: (1) to predict the aerodynamic performance or power production of the turbine, and (2) to predict the detailed time-varying distribution of aerodynamic loads acting on the turbine rotor blades. In general, the same models are used to accomplish both objectives. Accurate prediction of turbine aerodynamic performance does not guarantee accurate prediction of the loading distribution—the performance predictions result from the integration of time-averaged aerodynamic lift and drag over the entire turbine, and significant errors may be present in the detailed lift and drag predictions but balance out in the performance predictions. Although there is a

considerable body of data showing good agreement of predicted performance with measured performance, especially for codes that have been tailored to give good results for the particular configuration of interest, there are very few data available against which to compare detailed load-distribution predictions. The aerodynamics of wind turbines are far too complex to model with simple formulas that can be solved with hand-held calculators; computer-based models ranging from very simplistic to very complex are required. Several commonly used aerodynamic models are described below.

22.2.1.1 Momentum Models

The simplest aerodynamic model of a horizontal-axis wind turbine is the actuator disk or momentum model, in which the turbine rotor is modeled as a single porous disk. This analysis was originally adapted for wind turbine use by Betz [9], from the propeller theory developed by Froude [10] and Lanchester [11]. To develop the equations for this model, the axial force acting on the rotor is equated to the time rate of change of the momentum of the air stream passing through the rotor. It is assumed that the mass of air that passes through the rotor disk remains separate from the surrounding air and that only the air passing through the disk slows down. That mass of air with a boundary surface of a circular cross-section, extended upstream and downstream of the rotor disk, is shown in Figure 22.10. No air flows across the lateral boundary of this *stream-tube*, so the mass flow rate of air at any position along the stream-tube will be the same. Because the air is incompressible, the decrease in the velocity of the air passing through the disk must be accompanied by an increase in the cross-sectional area of the stream-tube to maintain the same mass flow. The presence of the turbine causes the air approaching from the upstream to gradually slow down; thus, the velocity of the air arriving at the rotor disk is already lower than the free-stream windspeed. As mentioned above, this causes the stream-tube to expand. In addition, the static pressure of the air rises to compensate for the decrease in kinetic energy.

As the air passes through the rotor disk, there is a drop in static pressure; the air immediately downstream of the disk is below the atmospheric pressure level, but there is no instantaneous change in velocity. As the air continues downstream, the static pressure gradually increases until it again comes into equilibrium with the surrounding atmosphere, and the velocity drops accordingly. This region of the flow is referred to as the *wake*. Thus, the difference in flow conditions between the far upstream and the far wake is a decrease in kinetic energy, but there is no change in static pressure.

Utilizing conservation of mass, conservation of axial momentum, the Bernoulli equation, and the first law of thermodynamics, and assuming isothermal flow, the power produced by the turbine (the product of the axial force and the air velocity at the rotor) may be readily derived. From the conservation of axial

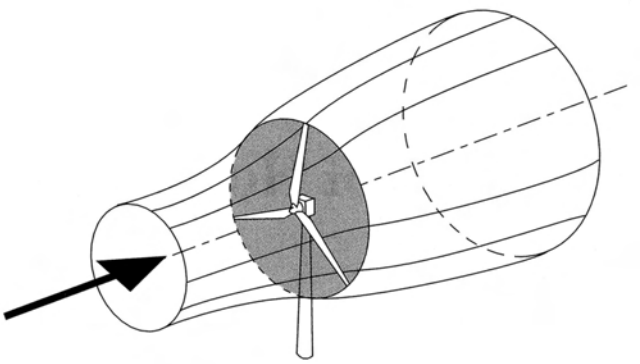

FIGURE 22.10 Schematic of stream-tube for horizontal-axis wind turbines.

momentum, the thrust on the rotor, T, may be expressed as

$$T = \dot{m}(U - v_w) = \rho A v(U - v_w), \tag{22.5}$$

where $\dot{m}$ is the mass flow rate of air ($\dot{m} = \rho A v$), v is the wind velocity at the rotor disk, v_w is the wind velocity far downstream of the rotor disk (in the wake), and A is the area of the rotor disk.

The thrust may also be expressed in terms of the pressure drop caused by the rotor:

$$T = A(p_u - p_d), \tag{22.6}$$

where p_u is the pressure just upwind of the rotor disk and p_d is the pressure just downwind of the rotor disk.

The Bernoulli equation, applied just upwind of the rotor and just downwind of the rotor, yields

$$p_\infty + 1/2\rho U^2 = p_u + 1/2\rho v_u^2, \tag{22.7}$$

$$p_d + 1/2\rho v_d^2 = p_w + 1/2\rho v_w^2. \tag{22.8}$$

Far upwind of the rotor and far downwind of the rotor, the pressures are equal ($p_\infty = p_w$), and the velocity is the same just upwind and just downwind of the rotor ($v_u = v_d$). Substituting Equation 22.7 and Equation 22.8 into Equation 22.6 and using the above equalities yields

$$T = A[(1/2\rho U^2 - 1/2\rho v_u^2) - (1/2\rho v_d^2 - 1/2\rho v_w^2)] = 1/2\rho A(U^2 - v_w^2). \tag{22.9}$$

Equating Equation 22.5 and Equation 22.9 then yields

$$v = 1/2(U + v_w). \tag{22.10}$$

That is, the velocity at the rotor disk is equal to the mean of the free-stream and wake velocities; thus, the velocity change between the free-stream and the wake is twice the change between the free-stream and the disk.

The power produced at the rotor, assuming isothermal flow and ambient pressure in the wake and utilizing Equation 22.10, is

$$P = Tv = 1/2\rho A(U^2 - v_w^2)v, = 1/2\rho A(U - v_w)(U + v_w)v, = 1/2\rho A[2(U - v)]2vv,$$

$$= 2\rho A(U - v)v^2. \tag{22.11}$$

Now, define

$$a = (U - v)/U$$

which is commonly known as the *axial interference factor*. Rearranging, Equation 22.11 becomes

$$P = 2\rho A(aU)(1 - a)^2 U^2 = 2\rho A U^3 a(1 - a)^2. \tag{22.12}$$

The power coefficient for the turbine, then, is

$$C_p = 4a(1 - a)^2. \tag{22.13}$$

This is maximized at $a = 1/3$, yielding $C_{p,max} = 16/27 = 0.593$ as the maximum possible performance coefficient for a lift-type machine, a maximum often referred to as the *Betz limit*. Expressed in slightly

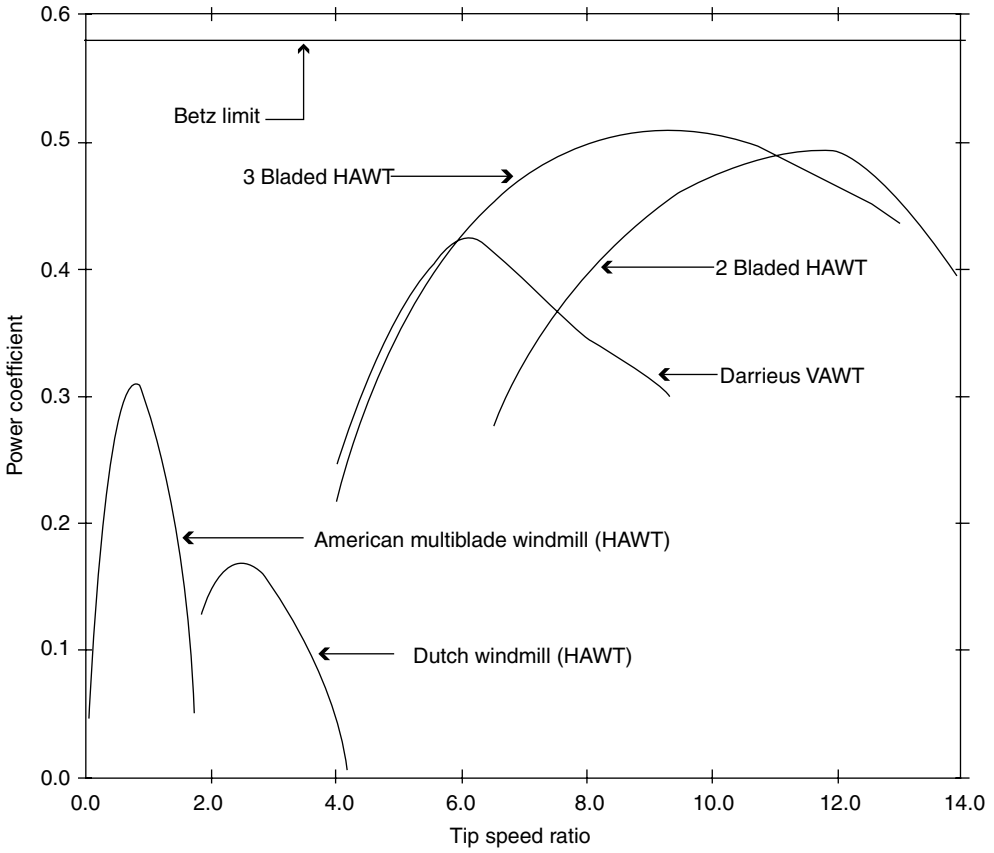

FIGURE 22.11 Typical performance of various types of wind turbines.

different terms, no lift-type turbine can extract more than 59.3% of the energy available in the wind passing through the rotor.

The typical performance of various types of wind machines is compared to the Betz limit in Figure 22.11, where the variations of the turbine power coefficients with the tip-speed ratio (the ratio of the speed of the blade tip to the free-stream windspeed) are presented. Even though the maximum performance of modern HAWTs and VAWTs is well above that of the older, drag-type machines such as the Dutch windmill and the American multiblade windmill, it is still somewhat below the Betz limit. Some HAWTs have demonstrated peak performance coefficients approaching 52%.

For horizontal-axis wind turbines, the momentum model can be expanded to the widely used blade element momentum (BEM) model in which the blades are divided into small radial elements and local flow conditions at each element are used to determine blade forces and loads on those elements. To obtain accurate predictions, this model typically incorporates numerous modifications to account for blade and turbine wake effects, the three-dimensional flow near blade tips, the thick blade sections near the root, and blade stall at high windspeeds. Additional information on these models may be found in Hansen and Butterfield [12], Wilson [13], and Snel [14].

A very similar derivation yields a momentum model for the vertical-axis wind turbine. This model may be expanded into the multiple stream-tube model (the turbine rotor is modeled as multiple actuator disks, rather than just one) and the double-multiple stream-tube model (multiple actuator disks, with separate ones modeling the upwind and downwind passes of the rotor blades) that are the VAWT

equivalent of the HAWT blade element model. Additional information on these models may be found in Touryan et al. [15], Wilson [13], and Paraschivoiu [16].

Momentum-based models are extremely popular with wind turbine designers because they are simple, fast, and fairly accurate for performance prediction, especially after they are tuned for a particular configuration. However, they are approximate because they are based upon the assumptions of flow conditions that are fixed in time and space. They cannot predict the effects of yawed flow, unsteady aerodynamics, and other complex flows that are present on wind turbines, all of which can have large impacts on turbine performance and loads. In some cases, specialized codes based on experimental results are used to model some of these effects, but these codes are limited to specific turbine sizes and geometries. In other cases, more realistic models, such as vortex-based models, full computational fluid dynamics (CFD) models, and hybrid models, are used to estimate these effects.

22.2.1.2 Vortex Models

Vortex models are usually more properly referred to as lifting line or lifting surface models, depending on whether a lifting line or a lifting surface formulation is used to model the blades. In the lifting line method, each rotor blade is modeled as a series of segmented "bound line vortices" located at the blade ¼-chord line, as illustrated in Figure 22.12a. Line-vortex strengths, defined by the blade lift at each radial location, are associated with the vortex line segments. The lifting surface method represents the blade in more detail, as a distribution of vortex line segments over the blade surface, as illustrated in Figure 22.12b. Either of these models will generate both trailing vorticity (perpendicular to the span of the blade) due to the differences in vortex strength along the blade span and shed vorticity (parallel to the span of the blade) due to time-dependent changes in vortex strength, that are shed into the wake as the turbine rotates. These vortex methods lend themselves to the modeling of unsteady problems, as the shed vorticity models the time-dependent changes in the blade bound vortex strength. Solutions are achieved by impulsively starting the turbine in a uniform flow field and allowing the computational flow field to develop until it reaches a steady state or periodic condition.

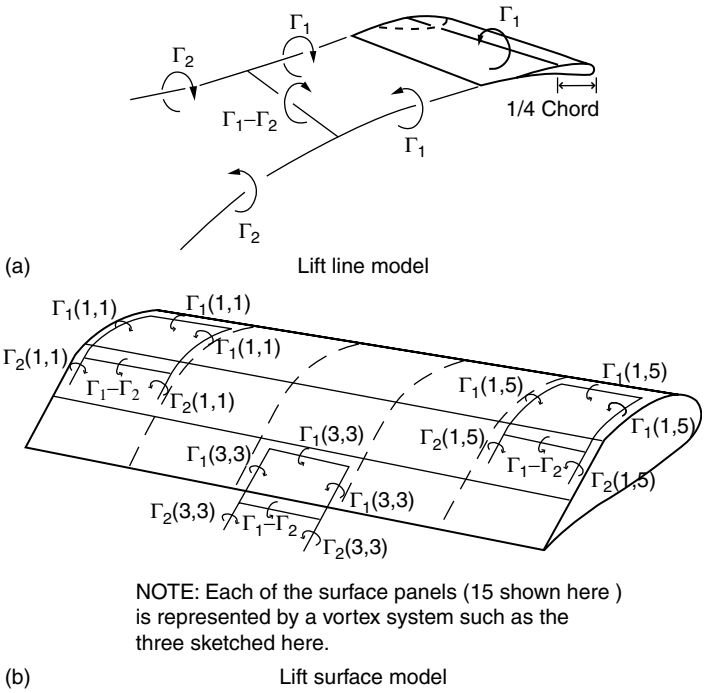

FIGURE 22.12 Schematic of lifting line and lifting surface models of turbine blades.

The manner in which the transport of the vorticity in the turbine wake is modeled depends on whether a free-wake or a fixed-wake (or prescribed-wake) model is used. In the free-wake model, the vorticity is allowed to convect, stretch, and rotate as it is transported through the wake. However, the movement of each line vortex is influenced by the presence of all of the other line vortices, including those on the blade. As the computation progresses in time, the number of vortices that must be followed and the time required to calculate the vortex interactions both grow very quickly. To minimize the need for large computer resources, the fixed or prescribed wake models have been developed. In these models, the geometry of the wake is either fixed or described by only a few parameters, and the vortex interactions in the wake are no longer directly calculated. The result is a much faster execution time, but the accuracy of the predicted power generation and blade loads depends very heavily upon the fidelity with which the specified wake approximates the actual physical wake. The three-dimensional, lifting-surface, free-wake formulation is the most physically realistic of the vortex models, but a computer program implementing such a model will require a large amount of computer resources and time. Experience has shown that the dramatic increase in computer resources required by such a model does not yield significantly more accurate predictions than what can be obtained with a three-dimensional, lifting-line, free-wake model. A major problem with vortex codes is the difficulty in finding a good balance between model simplification (and the associated limitations on fidelity), computation time, and desired accuracy. Vortex models are not widely used in the wind industry today; they are much more expensive in terms of computer resources than momentum models, and they are less accurate than computational fluid dynamics models. Additional information on vortex models for both HAWTs and VAWTs may be found in Kocurek [17], Snel [14] and Strickland et al. [18], among others.

22.2.1.3 Limitations Common to the Momentum and Vortex Models

Both momentum-based and vortex models normally utilize airfoil performance characteristic tables (lift and drag coefficients as functions of angle of attack, such as are shown in Figure 22.8), and air velocity to determine the blade lift and drag. These tables are generated from static two-dimensional wind tunnel test results or two-dimensional static airfoil design code predictions. The contents of the tables are modified with empirical, semiempirical, or analytic methods and used to estimate blade loads under the three-dimensional, dynamic conditions actually experienced by the turbine blades. The greatest difficulty in obtaining accurate load distribution predictions with either the momentum models or the vortex models is the challenge of accurately determining the appropriate airfoil performance characteristics.

22.2.1.4 Computational Fluid Dynamics Models

Computational fluid dynamics (CFD), in a broad sense, is the solution to the partial differential equations describing the flow field by approximating these equations with algebraic expressions (discretizing them), and then solving those expressions numerically with the aid of a computer. Within the wind energy community, the term CFD normally refers to the numerical solution of the unsteady Reynolds-averaged Navier–Stokes (RaNS) equations [19,20], often restricted to four partial differential equations (one conservation of mass equation, and conservation of momentum equations in three orthogonal directions) that describe general ideal-gas, incompressible, nonreacting fluid flow.

One might argue that the most detailed and physically realistic method of predicting the performance of and loads on a wind turbine is to utilize CFD to model the airflow around the turbine and through the rotor, calculating the airfoil lift and drag directly. The flow field in the vicinity of the wind turbine is approximated as a computational grid of variable density, and the discretized Navier–Stokes equations are applied to each element of that grid. The computational grid close to the turbine blades must be very, very dense to capture the details of the airflow around the blades; it becomes less dense as the distance from the blades becomes greater and the effect of the blades on the airflow decreases. The resulting set of simultaneous equations must be solved, frequently in a time-marching manner, to determine the time-dependent nature of the entire flow field.

Duque et al. [21] describe a fairly recent CFD investigation of a wind turbine in which they utilized a complex grid with 11.5 million points to model the flow around a 10-m diameter HAWT rotor and tower combination. A steady-flow solution (rotor facing directly into the wind) for that model at a single windspeed, utilizing eight PC processors, each operating at 1.4 GHz in a parallel processor computer configuration, required approximately 26 h. An unsteady-flow solution (rotor yawed at an angle to the wind) with the same computing resources required over 48 h for each rotor revolution. Sørensen et al. [22] and Johansen et al. [23] report other recent CFD modeling efforts.

At this point, CFD is suitable for research use or final design verification only—it is far too slow and requires far too many computer resources to be considered for use as a routine design tool. CFD also suffers from some shortcomings that limit its accuracy in performance and loads calculations. First, it does not consistently yield highly accurate results for airfoil lift and drag because it cannot adequately model the transition of flow over the airfoil surface from laminar, well-ordered, basically two-dimensional flow, to inherently three-dimensional and unsteady turbulent flow that is accompanied by rapid fluctuations in both velocity and pressure. Most wind turbines today utilize airfoils that will experience such a transition in the flow. Second, most CFD models today cannot adequately predict the effects of separated flow, especially three-dimensional separated flow, such as will occur near the hub of the wind turbine rotor under most operating conditions. In spite of these limitations, CFD calculations, when used wisely, can often yield much useful information. Efforts to improve the accuracy of CFD calculations continue.

22.2.1.5 Hybrid Models

The hybrid model approach typically approximates the airflow close to the turbine with the discretized Navier–Stokes equations, similar to the procedure used by the CFD models. However, away from the turbine, the model uses nonviscous or potential flow equations that are much less complex and that can be solved much faster than the Navier–Stokes equations. The two solutions must be merged at the boundary between the two regions. The result is a code with the accuracy of the CFD model, but one that requires an order of magnitude less computing resources to solve. Xu and Sankar [24] describe recent work on such a code. However, even this hybrid model requires a large amount of computer resources and is too slow and expensive to be considered a practical design tool.

22.2.1.6 Model Results

None of these aerodynamic models is capable of accurately predicting the performance of and detailed loads on an arbitrary wind turbine operating at a variety of windspeeds. To have high confidence in the code predictions for a turbine design, the code must be calibrated against the measured performance and loads obtained from turbines of similar size and shape. Simms et al. [25] report on the ability of 19codes based on the above models to predict the distributed loads on and performance of an upwind HAWT with a 10-m diameter rotor that was tested in the NASA/Ames 80 ft. $\times$120 ft. (24.4 m$\times$36.6 m) wind tunnel. Although the rotor was small compared to the 80-m diameter and larger commercial turbines that are being built today, a panel of experts from around the world concluded that it was large enough to yield results representative of what would be observed on the larger turbines. The comparisons of the code predictions and the experimental results were, in general, poor; turbine power predictions ranged from 30 to 275% of measured values, and blade-bending moment predictions ranged from 85 to 150% of measured values for what is considered to be the most easy-to-predict conditions of no yaw, steady state, and low windspeed. Many aerodynamic code developers have spent considerable effort over the years since that comparison attempting to identify the sources of the discrepancies and improving the accuracy of their various codes.

Additional information and references on wind turbine aerodynamics models may be found in Hansen and Butterfield [12], Wilson [13], and Snel [14] for HAWTs, and in Touryan et al. [15] and Wilson [13] for VAWTs.

Most wind turbine companies today continue to use the very fast momentum-based models for design purposes, in spite of the approximations and inaccuracies that are inherent in these models. The analysts

doing the studies tweak these models to get good comparison with measurements from an existing turbine, and then use them to predict performance and loads for new turbines that are fairly close in size and geometry to the existing turbine. If the new turbine is significantly different in size and shape from the reference turbine, the performance predictions are considered to be subject to considerable error. Performance tests on prototype turbines are required to define the actual performance and loads.

22.3 Wind Turbine Loads

Wind turbines are fatigue-driven structures; they normally fail not as the result of a single application of a large-amplitude load, but as a result of the repeated application and removal (or cycling) of small-amplitude loads. Each load cycle causes microscopic damage to the structure, and the accumulated effect of many cycles of varying amplitude eventually leads to failure of the structure, a process referred to as *fatigue failure*. In general, the smaller the amplitude of the load, the larger the number of load cycles the structure can withstand before failing. Therefore, it is very important that the loads acting on a wind turbine be well understood.

The wind is random or stochastic in nature, with significant short-term variations or turbulence in both direction and velocity. Wind turbine aerodynamic loads may fall into one of two broad categories. One category consists of the deterministic loads occurring in narrow frequency bands resulting from the mean steady atmospheric wind, wind shear, rotor rotation, and other deterministic effects. The other category consists of the random loads occurring over all frequencies resulting from the wind turbulence. As recently as 10–12 years ago, the deterministic loads were frequently predicted with an aerodynamics code, such as those described earlier, utilizing a uniform wind input, while the random loads were estimated with empirical relations. However, turbine designers now recognize that this approach may lead to serious under prediction of both the maximum and random blade loads, resulting in costly short-term component failures. Most analysts today utilize an aerodynamics performance code with a wind model that includes a good representation of the turbulence of the wind in all three dimensions to predict long-term wind turbine loads. The appropriate method of determining the wind-induced extreme events and random loads that limit the lifetime of a turbine remains the subject of ongoing research. This lack of knowledge of loads is typically compensated for in the design process by incorporation of large safety margins, leading to excess material and cost. Civil engineers have spent decades developing statistical methods for predicting wind and wave loads on offshore drilling platforms to help reduce the cost and increase the reliability of those platforms. The wind turbine industry is just now starting to apply that technology to predict the wind loads on land-based wind turbines.

22.4 Wind Turbine Structural Dynamic Considerations

Input loads and dynamic interactions result in forces, moments, and motions in wind turbines, phenomena referred to as structural dynamics. By applying various analytical methods, the impact of changes in turbine configurations, controls, and subsystems on the behavior of the turbine can be predicted. General wind turbine structural dynamic concerns and methods of analysis are discussed in the following paragraphs.

22.4.1 Horizontal-Axis Wind Turbine Structural Dynamics

Small-horizontal-axis turbine designs usually use fairly rigid, high-aspect-ratio (the blade length is much greater than the blade chord) blades, cantilevered from a rigid hub and main shaft. As turbine size increases, the flexibility of the components tends to increase, even if the relative scales remain the same, so the blades on larger turbines tend to be quite flexible, and the hub and main shaft tend to be far less rigid than corresponding components on small turbines. The entire drivetrain assembly is mounted on and yaws about a tower that may also be flexible. These structures have many natural vibration modes

and some of them may be excited by the wind or the blade rotation frequency to cause a resonance condition, amplifying vibrations and causing large stresses in one or more components. Operating at a resonance condition can quickly lead to component failure and result in the destruction of the turbine. Careful structural analysis during the turbine design may not guarantee that the turbine will not experience a resonance condition, as analysis techniques are not infallible, but ignoring the analysis altogether or failing to properly conduct parts of it may dramatically increase the probability that the turbine will experience one or more resonance conditions, leading to early failure. Although the relatively rigid small turbines are not likely to experience these resonance problems, the very flexible, highly dynamic, larger turbines may well experience resonance problems unless they are very carefully designed and controlled. Turbines that operate over a range of rotational speeds (variable-speed turbines) are especially challenging to design. The designer will usually try to minimize the number of resonances that occur within the operational speed range, and then implement a controller that will avoid operating at those resonance conditions. The actual resonances typically depend on the rotor speed, and the severity of the resonance depends on the windspeed, so the controller logic can become quite complicated.

The large relative motion between the rotor and the tower frequently precludes the use of standard commercial finite-element analysis codes and requires the use of a model constructed specifically for analysis of wind turbines. Development of such a model can be a rather daunting task, as it requires the formulation and solution of the full nonlinear governing equations of motion. The model must incorporate the yaw motion of the nacelle, the pitch control of the blades, any motion and control associated with hinged blades, the time-dependent interaction between the rotor and the supporting tower, etc. If the full equations of motion are developed with either finite-element or multibody dynamics formulations, the resultant models contain moderate numbers of elements and potential motions (or degrees of freedom, DOF), and significant computer resources are required to solve the problem. On the other hand, a modal formulation utilizing limited DOF may be able to yield an accurate representation of the wind turbine, resulting in models that do not require large computing resources. The development of the modal equations of motion may require somewhat more effort than do the finite-element or multibody equations, and the equations are apt to be more complex. The modal degrees of freedom must include, at a minimum, blade bending in two directions, blade motion relative to the main shaft, drive train torsion, tower bending in two directions, and nacelle yaw. Blade torsion (twisting about the long axis) is not normally included in current models, but it may become more important as the turbine sizes continue to increase and the blades become more flexible. The accuracy of some modal formulations is limited by their inability to model the direction-specific, nonlinear variation of airfoil lift with angle of attack that occurs as a result of aerodynamic stall. However, this is not an inherent limitation of the technique, and some formulations are free of these limitations. The modal formulation is the most widely used HAWT analysis tool today, but, as computer resources become more readily available, the more accurate finite-element (such as Abaqus [26]) and multibody dynamic codes (such as Adams [27]) will certainly become more widely used.

It is possible to develop techniques in the frequency domain to analyze many aspects of the turbine dynamics. The frequency domain calculations are fast, but they can only be applied to linear, time-invariant systems and, therefore, cannot deal with some important aspects of wind turbine operations such as aerodynamic stall, start-up and shutdown operations, variable speed operation, and nonlinear control system dynamics. In spite of these limitations, frequency domain solutions of modal formulations are frequently used in the preliminary design of a wind turbine, when quick analysis of many configurations is required. Regardless of the methods used in preliminary design, the state of the art in wind turbine design today is to use highly detailed modal, lumped-mass, or finite-element-based equations of motion, coupled with time-accurate solutions, to analyze the turbine behavior for the detailed final design calculations.

Malcolm and Wright [28] and Molenaar and Dijkstra [29] provide reviews of some of the available HAWT dynamics codes that have been developed, together with their limitations. Buhl et al. [30] compare some of the HAWT dynamics codes that have been extensively verified and that are widely used

today, and Quarton [31] provides a good history of the development of HAWT wind turbine analysis codes. More general finite-element dynamics codes are described by others [32–35].

22.4.2 Vertical-Axis Wind Turbine Structural Dynamics

Darrieus turbine designs normally use relatively slender, high-aspect-ratio structural elements for the blades and supporting tower. As with large HAWTs, the result is a very flexible, highly dynamic structure, with many natural modes of vibration that again must be carefully analyzed to ensure that the turbine will avoid structural resonance conditions under all operating environments. The guy cables and turbine support structure can typically be analyzed with commercial or conventional finite-element codes, but the tower and blades require a more refined analysis, usually requiring the use of a finite-element code possessing options for analyzing rotating systems. With such a code, the blades and tower of a VAWT are modeled in a rotating coordinate frame, resulting in time-independent interaction coefficients. The equations of motion must incorporate the effects of the steady centrifugal and gravitational forces, the aerodynamic forces due to the turbulent wind, and the forces arising from rotating coordinate system effects. Detailed information on finite-element modeling of VAWTs may be found in Lobitz and Sullivan [36].

22.5 Peak Power Limitation

All turbines incorporate some method of regulating or limiting the peak power produced. The entire turbine, including the rotor, the transmission and the generator, must be sized to handle the loads associated with peak power production. While high winds (above, for example, 25 m/s) contain large amounts of available power, they do not occur very often, and the power that can be captured is very small. This is illustrated in Figure 22.13 for the Amarillo, Texas airport. In this figure, the power density is the power per unit of rotor area (normalized to yield a value under the curve of unity) that is available for capture by a wind turbine. This takes into account the amount of time that the wind actually blows at each windspeed (the probability density that is also shown on the figure). Amarillo occasionally

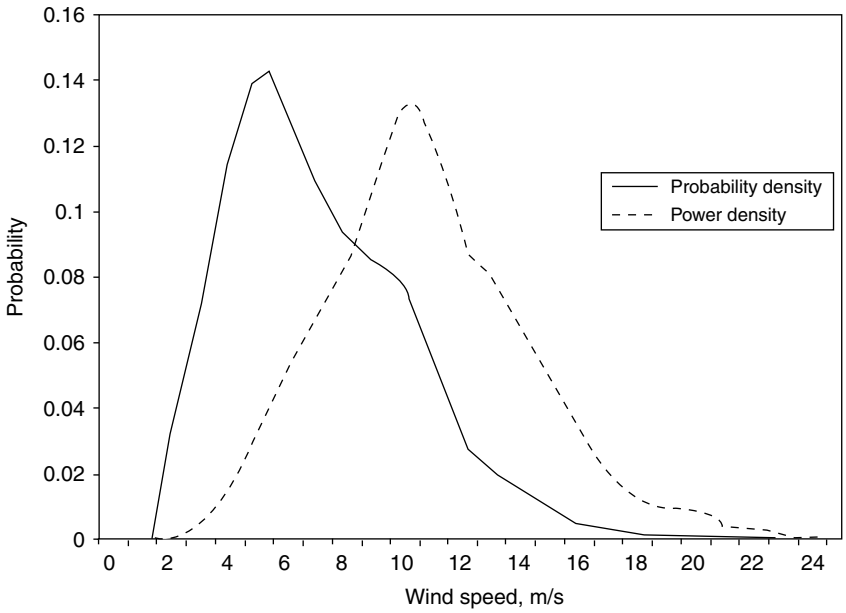

FIGURE 22.13 Windspeed and wind power probability densities for Amarillo, Texas airport.

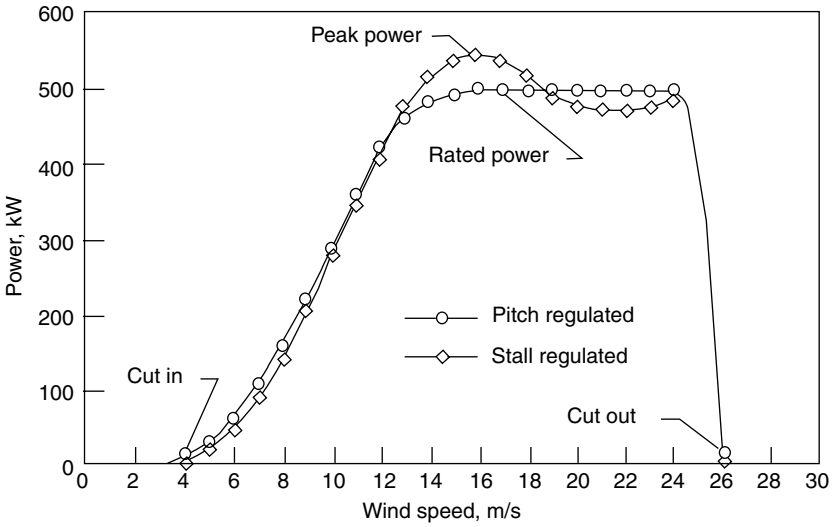

FIGURE 22.14 Sample power curves for stall-regulated and pitch-regulated wind turbines.

experiences very high winds, but as seen from this probability density, they do not occur very often, and the energy that could be captured from winds above 25 m/s is negligible.

Generators and transmissions operate most efficiently at their design conditions, typically close to their maximum capacity. These efficiencies drop off quickly at conditions below design. Cost trade-off studies reveal that it is far more cost effective to limit the maximum power level to that achieved at, for instance, 13–14 m/s and to shut the turbine down completely at a cutout windspeed of, for example, 26 m/s, as illustrated in Figure 22.14, than to try to capture the maximum amount of power at the higher windspeeds. Under these conditions, the transmission and generator are operating near design conditions for a significant portion of the time, and the turbine can be built with far less material than would be required for a turbine that generates peak power at 25 m/s. The additional energy captured due to the increase in generator and transmission efficiencies at the lower windspeeds is usually many times greater than that lost due to limiting the peak power at the rather infrequent winds above 14 m/s (refer to the windspeed distribution in Figure 22.13).

Nearly all modern large horizontal-axis turbines now use blade pitch control, where either the entire blade or a portion of it is rotated about the longitudinal axis to change the angle of attack and, therefore, the power output of the turbine, to limit peak power. Some turbines are designed with fixed-pitch blades, and rely on airfoil stall at high winds to limit the maximum power output of the machine. Small turbines frequently incorporate passive features, such as tail vanes and furling, that turn the rotor so the rotor axis is no longer aligned with the wind, to limit peak power production in high winds.

With full-span blade pitch control, the blade may be rotated about its longitudinal axis to decrease the effective angle of attack as the windspeed increases (commonly referred to as *pitch-to-feather*), causing decreased blade lift and limiting the peak power at the desired level. Alternatively, the blade may be rotated about that axis to increase the effective angle of attack (commonly referred to as *pitch-to-stall*), causing blade stall and limiting peak power. Although pitch-to-feather control results in decreased drag loads at high winds, a major disadvantage is poor peak power control during high-wind stochastic conditions—sudden increases in windspeed will result in corresponding increases in angle of attack, loads, and power generation. Power excursions can exceed twice the rated power levels before the high-inertia blade pitch system can compensate for the windspeed increases. Blade stall control (either fixed-pitch or pitch-to-stall), on the other hand, results in better peak power control at high winds. Major disadvantages of stall control include increased blade drag loads as the windspeed increases (even after

stall) and possible large dynamic loads due to wind turbulence. A major advantage of fixed-pitch stall control is the lower cost compared to the active pitch control. Sample power curves for fixed-pitch stall- and pitch-regulated (pitch-to-feather) 500-kW turbines are shown in Figure 22.14. The average peak power cannot be as well regulated with fixed-pitch stall control as with either pitch-to-feather or pitch to stall control.

The use of only a portion of the airfoil surface (typically including the blade tip) as a control surface is referred to as "partial-span" control. Adjusting the pitch (and, thus, the lift and drag) of this portion of the blade independently of the remainder of the blade is used to control the peak power output of the turbine. These control surfaces are usually much smaller than the full blade, so they can respond to wind changes much faster than can the full-span blade. However, partial-span devices are very difficult to integrate into a blade, and the gaps around the devices tend to generate noise. Some recent research has investigated the use of very small load control devices that can generate large changes in lift and drag while experiencing small loads. Dimensions of these devices are typically on the order of 1% of the blade chord; their small size means they can be activated very quickly to alleviate excess loads and they are less likely to create large amounts of noise. Mayda et al. [37] discuss the use of CFD to investigate the effects of some of these devices.

Several other methods of pitch control have also been used, but on a limited basis. Passive pitch control techniques automatically adjust the blade pitch angle by using cams activated by centrifugal loads or by using tailored blade materials that permit the blade to twist toward feather or stall under high loads. These devices are very carefully tailored to maintain peak performance at lower windspeeds, but limit the peak power and blade loads at high windspeed.

Most vertical-axis wind turbines utilize stall regulation with fixed-pitch blades to control peak power, but some straight-bladed VAWTs are equipped with full-span pitch controls.

22.6 Turbine Subsystems

The wind turbine incorporates many subsystems, in addition to the actual turbine, to generate power. The electrical power generation, yaw, and controls systems are the only ones that will be discussed here.

22.6.1 Electrical Power Generation Subsystem

Once a wind turbine has converted the kinetic energy in the wind into rotational mechanical energy, that rotational energy is usually converted by a generator into electricity that can be readily transported to where it is needed. In most cases, the generator requires an input shaft speed that is much higher than the turbine shaft speed. These speeds are matched by a step-up transmission that increases the turbine shaft speed to that required by the generator.

While some wind turbines utilize permanent magnet alternators or generators, most grid-connected turbines today utilize either synchronous or induction generators. Synchronous generators are more complex and tend to be more expensive than induction generators, but they provide excellent voltage and frequency control of the generated power, and can deliver reactive power to the grid. However, these generators are not intrinsically self-starting (the blades are usually pitched to start the turbine), do not provide powertrain damping, and require sophisticated controls for connecting to the grid, as the output frequency (and, thus, the speed of the generator) must be precisely matched to the grid frequency before this may be accomplished.

Induction generators have a simple, rugged construction, they may readily be used as motors to spin a turbine up to speed, they are cheaper than synchronous generators, they may be connected to and disconnected form the grid relatively easily, and they provide some powertrain damping to smooth out the cyclic torque variations inherent in the wind turbine output. However, they require reactive power from either power electronics or the grid, and they can contribute to frequency and voltage instabilities in the grid to which they are connected. These adverse effects can usually be solved fairly quickly and at low

cost with modern power electronics. Induction generators are, therefore, the most common type found on wind turbines.

Other types of generators, though less common, are also used on wind turbines. Permanent magnet generators eliminate the need for windings or winding current to provide the magnetic field, leading to a simple, rugged construction. The power produced by this type of generator is usually variable voltage and frequency AC that must be converted to DC or to fixed voltage and frequency AC with power electronics. Even with the addition of power electronics, these machines tend to achieve higher efficiency at low-power ratings than either induction or synchronous generators, leading to increased energy capture, but the technology is less mature for permanent magnet generators than it is for other types of generators. Although the cost of these generators has, historically, been somewhat higher than that of induction or synchronous generators, recent advances in technology have resulted in price decreases, making the technology quite competitive with the older technologies, and they are becoming more common. Fuchs et al. [38] describe the development of a permanent magnet generator for wind turbine use.

Direct drive generators are normally synchronous machines (with either conventional or permanent magnet excitation) of special design, built with a sufficient number of poles to permit the generator rotor to rotate at the same speed as the wind turbine rotor. This eliminates the need for a gearbox or transmission. These generators are usually used in conjunction with power electronic converters to decouple the generator from the network and provide flexibility in the voltage and frequency requirements of the generator.

Most older turbines operate at a single, fixed rotational speed, but many newer turbines, and especially the large ones, are variable-speed, operating within a fixed range of rotational speeds. Variable-speed turbine operation offers several major advantages over fixed-speed operation:

1. The aerodynamic efficiency of the rotor at low to moderate windspeeds may be improved by changing the rotational speed to keep the turbine operating close to the optimum tip-speed ratio, maximizing the power coefficient. As explained earlier, at higher windspeeds, the blades are either in stall or are pitched to limit peak power. The rotor speed may also be adjusted to fine-tune peak power regulation.
2. System dynamic loads may be attenuated by the inertia of the rotor as it speeds up and slows down in response to wind gusts.
3. The turbine may be operated in a variety of modes, including operation at maximum efficiency to maximize energy capture at lower windspeeds, and operation to minimize fatigue damage.

As mentioned earlier, for variable-speed operation, certain rotational speeds within the operating-speed range will likely excite turbine vibration modes, causing structural resonance and increased rates of fatigue damage. These rotational speeds must be avoided during operation, leading to complex control schemes.

Variable-speed operation is possible with any type of generator. In general, variable-speed operation results in variable-frequency/variable-voltage AC power. Interfacing the turbine to the power grid (a very common application) requires this power be converted to high quality, constant frequency power. Several methods have been developed for accomplishing this with sophisticated power electronics (see Smith [39], for example), but research to develop improved methods with higher efficiencies continues. Manwell et al. [40] give a brief overview of some common types of power converters and provide references for more extensive discussions of these devices.

Electrical generator efficiency tends to drop off rapidly as the generated power falls below the rated generator capacity, so single-generator wind turbine systems tend to be very inefficient at low windspeeds. Some turbine designs address this deficiency by incorporating multiple smaller generators. At low windspeed, only one generator might be attached to the drive train, with more being added as the windspeed increases. The net result is that each generator operates close to its rated power much of the time, increasing the overall generator efficiency. Similar increases in generator efficiency at low-power levels can be obtained with a single generator utilizing pole switching or multiple windings.

22.6.2 Yaw Subsystem

The rotor of a HAWT must be oriented so that the rotor axis is parallel to the wind direction for peak power production. While small turbines rely on passive systems, such as tail vanes, to accomplish this, most large, upwind HAWTs and a few downwind HAWTs incorporate active yaw control systems using a wind direction sensor and a drive motor/gear system to orient the rotor with respect to the wind direction. Some downwind HAWTs are designed to utilize the wind itself to automatically orient the rotor. Active yaw systems tended to be extremely problematical in early turbines, basically because the loads acting on them were not well understood. Yaw loads are much better understood today, and these systems are no longer a major problem area. VAWTs are not sensitive to wind direction and do not require yaw systems.

22.6.3 Controls Subsystem

One or more control systems are needed to integrate the operation of the many components of a wind turbine and to safely generate power. In a very general sense, a wind turbine control system consists of a number of sensors, a number of actuators, and a system of hardware and software that processes the signals from the sensors to generate signals to control the actuators. A turbine usually contains a minimum of two distinct controllers—a supervisory controller that handles the normal operation of the turbine, and a safety controller that will override the supervisory controller to bring the turbine to a safe state (usually stopped, with the brakes applied). Any particular turbine may incorporate many additional secondary or slave controllers, each of which handles only a limited number of tasks. An example of a secondary or slave controller would be a blade pitch controller that actually pitches the blade to follow a predetermined speed ramp during start-up or shutdown of the turbine and that regulates the power output of the turbine at the rated level in above-rated windspeed.

22.6.3.1 Supervisory Controller

The supervisory controller is usually computer or microprocessor-based and programmed with software to perform the controller functions. The basic turbine controller will start and stop the machine, connect or disconnect the generator output to the power grid, as needed, control the operation of the yaw and pitch systems (if present), perform diagnostics to monitor the operation of the machine, and perform normal or emergency shutdown of the turbine as required. For older turbines, the supervisory controller was frequently a fairly generic device with a minimum of machine-specific features that was simply added to an existing turbine. It would be programmed with either hardware or software modifications to implement the functions specific to that particular turbine. The controllers on newer turbines, especially large, variable-speed machines, incorporate much more intelligence than the old, generic type; they may be designed to utilize the pitch system to limit peak power and/or torque, to control the rotor speed, to maximize energy capture, to trade-off energy capture and loads mitigation, to reduce power fluctuations, to control power quality, and/or to actively control some turbine dynamics. Controllers with any or all of these capabilities are usually designed from scratch as an integral component of the wind turbine, and must be included in the models of system aerodynamics and structural dynamics to obtain accurate estimates of loads and motions.

22.6.3.2 Safety Controller

The safety controller acts as a backup to the supervisory controller, and takes over if the supervisory controller fails to maintain the turbine in a safe operating mode. It is normally triggered by the activation of certain safety sensors, such as excessive vibration, excessive rotor speed, or excessive generator power, that are independent of the sensors connected to the supervisory controller, but it may also be activated by an operator-controlled emergency stop button. This system must be as independent from the main control system as possible, and must be designed to be fail-safe and highly reliable, since it may be the last line of defense to save a turbine from self-destruction. The safety

controller will normally consist of a hard-wired, fail-safe circuit monitoring a number of sensors. If any of the sensors indicates a problem, the safety controller takes control and ensures that the turbine is brought to a safe condition. This might include, for example, de-energizing all electrical systems, pitching the blades to the feather position, and engaging the spring-applied emergency brakes (that are held off in normal operation).

22.7 Other Wind-Energy Conversion Considerations

The actual turbine system is the single most important and most costly item of a wind energy conversion system, but there are many other aspects of the system that must be considered and carefully optimized before wind energy can be produced at a cost competitive price. These aspects include things like turbine siting, installation and foundations, operating and maintenance costs, manufacturing processes, transport of components to the site, turbine payback period, dependence of wind energy COE on turbine size, and environmental concerns. Turbine siting has already been discussed in Section 18.2. This chapter will only discuss materials, installations, costs, and environmental concerns. Additional information, including extensive reference lists, on all of these aspects can be found in Refs. [40–42].

22.7.1 Wind Turbine Materials

As mentioned earlier, wind turbines are fatigue-critical structures (their design is driven by consideration of the cyclic fatigue loads they must endure), and the number of fatigue cycles they experience in a 20–30 year design life is three orders of magnitude beyond the 10^6 cycles that has been the common limit of fatigue data for most materials. Most of the materials used in the construction of wind turbines are typical of those materials that are used in other rotating machinery and towers—relatively common structural materials such as metal, wood, concrete, and glass-fiber reinforced plastic (GFRP) composites. Towers are typically made of steel; a few have been built of concrete. Drive trains, generators, transmissions, and yaw drives are made of steel. These components can be readily designed so they experience very low stresses and will have a fatigue life of 20–30 years. Wind turbine blades, however, must be built with a minimum of lightweight material to minimize the gravity-induced cyclic loads on the blades, drivetrain, and tower. Over the past 15 years, high-cycle fatigue databases for many potential blade materials have been developed specifically for wind turbine applications. Mandell and Samborsky [43] and Mandell et al. [44] describe the main U.S. high-cycle fatigue database, while De Smet and Bach [45] and Kensche [46] describe the European counterpart. The material with the best all-around structural properties for wind turbine blades is carbon-fiber/epoxy composite. However, it is significantly more expensive than other potential materials. The blade material of choice today (and for the past decade or so) is GFRP, due to the high strength and stiffness that can be obtained, the ease of tailoring blades made of GFRP to handle the loads, and the relatively low cost of GFRP [47]. However, the trend towards larger and larger turbines, with the resultant increase in blade weight and flexibility, has created intense interest in utilizing some carbon fiber in the blades to decrease weight and add stiffness. The expense of carbon fiber, even in the cheapest form available today, means that turbine designers must incorporate it into blades in a cost-effective manner. According to Griffin [48] and Jackson et al. [49], one very efficient method of utilizing carbon fiber is to place it in the longitudinal spar caps, near the maximum thickness area of the blade, where its light weight and extra stiffness yield maximum benefits.

Obviously, the materials must be protected from the environment. Although paints and gel coats are adequate for most onshore installations, special care is required to protect turbine components from the extreme environment of offshore installations. This topic is beyond the scope of this chapter.

22.7.2 Wind Turbine Installations

Section 18.2 of this handbook discusses wind turbine siting considerations in some depth. Although individual turbines or small clusters of turbines may be used to provide power to small loads such as

FIGURE 22.15 Typical wind farm installation: New Mexico Wind Energy Center in Eastern New Mexico.

individual residences or businesses, the most common arrangement for producing large amounts of energy from the wind is to locate many wind turbines in close proximity to each other in a wind farm or wind park. Figure 22.15 is a photograph of several of the General Electric 1.5-MW turbines comprising the 204-MW New Mexico Wind Energy Center in eastern New Mexico (mentioned earlier in the case study in Section 18.2). Operating turbines in this manner leads to lower COE, as fixed construction costs, such as electrical grid interconnections and project development and management costs, and fixed maintenance costs, such as cranes, replacement parts and repair facilities, can be spread over a larger investment. The largest wind farms to date have capacity ratings in excess of 200 MW, and they consist of over 100 machines.

22.7.3 Energy Payback Period

A certain amount of energy is used in the manufacture, installation and eventual scrapping of any energy producing machine. The time required for the machine to generate as much energy as was used in its manufacture, installation and end of life scrapping is referred to as the energy payback period. Studies by Krohn [50] and Milborrow [51] show that the energy payback period of modern wind turbines ranges between 3 and 10 months, depending on the site windspeed and details of the turbine manufacture and installation. This payback period is among the shortest for any type of electricity production technology.

22.7.4 Wind Turbine Costs

Malcolm and Hansen [52], in a study performed for the U.S. Department of Energy, estimated the cost of wind turbines of four different sizes: 750 kW (46.6-m diameter rotor), 1.5 MW (66-m diameter rotor), 3.0 MW (93-m diameter rotor) and 5.0 MW (120-m diameter rotor). The hub height for each machine was 1.2 times the rotor diameter. These turbines were designed to operate in an 8.5-m/s annual average (at hub height) wind site, with a 50-year extreme 10-min windspeed of 42.5 m/s (International Electrotechnical Commission Class 2 site). The results are summarized in Table 22.1.

Although the intent of this study was strictly to look at the relative total turbine cost as a function of size, without regard to the actual turbine cost, the estimated cost for the 1.5-MW turbine was fairly close to actual turbine prices in 2002, the year of publication. Actual costs today are somewhat higher than those estimated by the study, due largely to increases in the cost of steel, the cost of concrete, the cost of

TABLE 22.1 Turbine Component Costs

Component\Rating	750 kW	1.5 MW	3.0 MW	5.0 MW
Rotor	**$101,897 (16%)**	**$247,530 (18%)**	**$727,931 (21%)**	**$1,484,426 (20%)**
Blades	10%	11%	13%	12%
Hub	3%	5%	6%	6%
Pitch mechanism and bearings	3%	3%	2%	2%
Drivetrain, nacelle	**$255,631 (39%)**	**$562,773 (40%)**	**$1,282,002 (37%)**	**$2,474,260 (33%)**
Low-speed shaft	1%	1%	2	2%
Bearings	1%	1%	1	1%
Gearbox	10%	11%	10	9%
Mechanical brake, HS coupling	<1%	<1%	<1%	<1%
Generator	7%	7%	6%	4%
Variable-speed electronics	8%	7%	6%	4%
Yaw drive and bearing	1%	1%	<1%	1%
Main frame	3%	5%	6%	6%
Electrical connections	5%	4%	4%	3%
Hydraulic systems	<1%	<1%	<1%	<1%
Nacelle cover	3%	3%	2%	2%
Control & safety system	**$10,000 (2%)**	**$10,200 (1%)**	**$10,490 (0.3%)**	**$10,780 (0.1%)**
Tower	**$66,660 (11%)**	**$183,828 (13%)**	**$551,415 (16%)**	**$1,176,152 (15%)**
Balance of station	**$217,869 (33%)**	**$388,411 (28%)**	**$873,312 (25%)**	**$2,458,244 (32%)**
Foundations	5%	4%	2%	1%
Transportation	4%	4%	7%	17%
Roads, civil works	7%	6%	4%	3%
Assembly and installation	4%	4%	3%	3%
Electrical interface/connections	11%	9%	7%	6%
Permits, engineering	2%	2%	2%	2%
Initial capital cost (ICC)	**$655,057**	**$1,392,741**	**$3,445,150**	**$7,603,862**
Normalized initial capital cost (ICC/Rating), ($/kW)	**873**	**928**	**1,148**	**1,520**
Annual energy production (AEP), (MWh)	**2,254**	**4,817**	**10,372**	**18,133**
Relative initial capital cost per kWh of energy produced	**1.01**	**1.00**	**1.15**	**1.45**

Source: From Malcolm, D. J. and Hansen, A. C. 2002. *WindPACT turbine rotor design study: June 2000–June 2002*, NREL/SR-500-32495, National Renewable Energy Laboratory, Golden, CO.

TABLE 22.2 Turbine Component Cost of Energy Contributions

Component\Rating	750 kW	1.5 MW	3.0 MW	5.0 MW
Rotor	11%	13%	16%	15%
Drive Train	27%	29%	28%	26%
Controls	1%	<1%	<1%	<1%
Tower	7%	9%	12%	12%
Balance of Station	23%	20%	19%	25%
Replacement Costs	11%	11%	9%	7%
O & M	18%	19%	17%	14%
Total COE (¢/kWh)	4.367	4.321	4.741	5.642

Source: From Malcolm, D. J. and A. C. Hansen. 2002. *WindPACT turbine rotor design study: June 2000–June 2002*, NREL/SR-500-32495, National Renewable Energy Laboratory, Golden, CO.

transportation, and the manufacturers' profit margins (resulting from the recent high demand for wind turbines).

Table 22.1, under "Balance of Station," shows that transportation costs increase dramatically as the size increases beyond 1.5 MW. This is due primarily to the difficulty of transporting the very large components over the highway. These costs would be significantly lower if the turbine could be shipped via ship or barge, but that is impossible for most onshore turbines. The table shows no advantage of scale on the initial capital cost, as that figure (in terms of $/kW) increases with turbine rating across the sizes studied. However, it does show that the annual energy production increases with rotor size to the power 2.2, due to the increase in tower height and the accompanying increase in windspeed arising from wind shear. The result is a minimum initial capital cost per generated kWh (ICC/AEP) for the 1.5-MW machine.

Malcolm and Hansen then estimated the cost of energy (COE) at a site with 5.8-m/s annual average winds at 10-m height, breaking the COE down by the contribution due to each major turbine component. The results are presented in Table 22.2. With current technology, it appears that the 1.5-MW turbine size actually has the lowest cost of energy. Keep in mind that the difference in COE for the three smaller turbines is relatively small; slight changes in the cost models could result in the lowest COE occurring for the 750-kW turbine or the 3.0-MW turbine rather than the 1.5-MW turbine. From these results, it is obvious that reductions in a single-component COE will not lead to dramatic changes in turbine COE. For example, the rotor contribution to the total COE is only 10%–16%, so a 20% decrease in the rotor contribution only yields a 2%–3% decrease in total COE. On the other hand, any improvement in a component that leads to increased turbine energy production may lead to a significant decrease in COE. A 20% increase in rotor energy capture at no additional capital or O&M cost, for example, would lead directly to a 20% decrease in COE.

22.7.5 Environmental Concerns

Although wind turbines generate electricity without causing any air pollution or creating any radioactive wastes, like all man-made structures, they do cause an impact on the environment. Wind turbines require a lot of land, but only about 5% of that land is used for turbine foundations, roads, electrical substations, and other wind-farm applications. The remaining 95% of the land is available for other uses such as farming or livestock grazing. Wind turbines do generate noise as well as electricity, but noise is seldom a problem with newer, large wind turbines. Some small turbines are quite noisy, but many of the newer ones are very quiet. Current industry standards call for characterization of turbine noise production and rate of decay with distance as part of the turbine testing process; therefore, noise information is readily available. Noise decreases quickly with distance from the source, so placing wind turbines appropriate distances from local homes has proven to be an effective means of eliminating noise as a problem. The noise level due to a typical, large, modern wind turbine, 300 m distant, is roughly comparable to the typical noise level in the reading room of a library.

22.7.5.1 Visual Impact

The visual impact of wind turbines is extremely subjective. What one person considers highly objectionable, another might consider as attractive or, at least, not objectionable. The relatively slow rotation of today's large wind turbines is viewed by most people as far less intrusive than the fast rotation of the early, small turbines. Visual impact can be minimized through careful design of a wind farm. The use of a single model of wind turbine in a wind farm and uniform spacing of the turbines helps alleviate concerns in this area. Computer simulation can be very helpful in evaluating potential visual impacts before construction begins.

22.7.5.2 Bird and Bat Collisions

One of the greatest environmental issues that the wind industry has had to face is the issue of bird deaths due to collisions with wind turbines. Concerns about this issue were, in large part, the result of relatively high numbers of raptor deaths in the Altamont Pass wind farms east of San Francisco, California in the 1980–1985 time frame. Dozens of studies of this issue have been conducted during the past 20 years. Sinclair and Morrison [53] and Sinclair [54] give overviews of the recent U.S. studies. One conclusion of the Altamont Pass studies is that the Altamont Pass situation is a worst-case scenario, due in large part to bad siting, and to the presence of overhead power lines that led to a large number of bird electrocutions. Colson [55] and Wolf [56] provide summaries of ways to minimize the impact of wind farms on birds. Among the specific recommendations are:

- Avoid bird migration corridors and areas of high bird concentrations(micro habitats or fly zones)
- Use fewer, larger turbines
- Minimize number of perching sites on turbine towers
- Bury electrical lines
- Conduct site-specific mitigation studies

In spite of the ongoing bird collision problems at Altamont Pass, the impact of wind energy on birds is very low compared with other human-related sources of bird deaths. According to the National Wind Coordinating Committee (NWCC), bird collisions with wind turbines caused the deaths of only 0.01%–0.02% of all the birds killed by collisions with man-made structures across the U.S. in 2001 [57]. Extrapolating their estimate of roughly two bird deaths per turbine per year to a scenario where 100% of U.S. electricity is provided by wind (and assuming a turbine size of 1.5 MW), yields an estimate of deaths due to collisions with wind turbines of 0.5%–1% of all bird deaths caused by collisions with structures. In contrast, bird collisions with buildings and windows account for about 55% of structure-related bird deaths, whereas collisions with vehicles, high-tension power lines, and communication towers account for about 17%.

Unexpectedly large numbers of bats have been killed by some wind farms in the eastern U.S. in the past few years. The wind industry has joined with Bat Conservation International, the U.S. Fish and Wildlife Service, and the National Renewable Energy Laboratory to identify and quantify the problem and to explore ways to mitigate these deaths. Several wind-energy companies are providing a portion of the funding for the cooperative effort that includes hiring a full-time biologist to spend three years coordinating the research effort. Efforts to resolve this issue are ongoing.

References

1. Shepherd, D. 1994. Historical development of the windmill, In *Wind Turbine Technology, Fundamental Concepts of Wind Turbine Engineering*, D. Spera, ed., ASME Press, New York, pp. 1–46.
2. Miley, S. J. 1982. A catalog of low Reynolds number airfoil data for wind turbine applications. RFP-3387. Department of Aerospace Engineering, Texas A&M University, College Station, TX.
3. Abbott, I. H. and von Doenhoff, A. E. 1959. *Theory of Wing Sections Including a Summary of Airfoil Data*. Dover Publications, New York.

4. Selig, M. S., Guglielmo, J. J., Broeren, A. P., and Giguere, P. 1995. *Summary of Low-Speed Airfoil Data*., *Vol. 1,* SoarTech Publications, Virginia Beach, VA.
5. Selig, M. S., Lyon, C. A., Giguere, P., Ninham, C. P., and Guglielmo, J. J. 1996. *Summary of Low-Speed Airfoil Data*., *Vol. 2,* SoarTech Publications, Virginia Beach, VA.
6. Lyon, C. A., Broeren, A. P., Giguere, P., Gopalarathnam, A., and Selig, M. S. 1997. *Summary of Low-Speed Airfoil Data*, *Vol. 3*,, SoarTech Publications, Virginia Beach, VA.
7. Selig, M. S. and McGranahan, B. D. 2004. Wind tunnel aerodynamic tests of six airfoils for use on small wind turbines; period of performance: October 31, 2002–January 31, 2003. NREL Report SR-500-34515. National Renewable Energy Laboratory, Golden, CO.
8. Somers, D. M. 1997. Design and experimental results for the S809 airfoil. SR-440-6918. National Renewable Energy Laboratory, Golden, CO.
9. Betz, A. 1920. Das maximum der theoretisch mőglichen ausnűtzung des windes durch wind-motoren. *Z. Gesamte Turbinewesen.*, 26.
10. Froude, R. E. 1889. On the part played in propulsion by differences of fluid pressure. *Transactions of the Institute of Naval Architects*, 30, 390–405.
11. Lanchester, F. W. 1915. A contribution to the theory of propulsion and the screw propeller. *Transactions of the Institute of Naval Architects*, 57, 98–116.
12. Hansen, A. C. and Butterfield, C. P. 1993. Aerodynamics of horizontal-axis wind turbines. *Annual Review of Fluid Mechanics*, 25, 115–149.
13. Wilson, R. E. 1994. Aerodynamic behavior of wind turbines, In *Wind Turbine Technology, Fundamental Concepts of Wind Turbine Engineering*, D. Spera, ed., pp. 215–282. ASME Press, New York.
14. Snel, H. 1998. Review of the present status of rotor aerodynamics. *Wind Energy*, 1, 46–69.
15. Touryan, K. J., Strickland, J. H., and Berg, D. E. 1987. Electric power from vertical-axis wind turbines. *Journal of Propulsion and Power*, 3, 6, 481–493.
16. Paraschivoiu, I. 2002. *Wind Turbine Design with Emphasis on Darrieus Concept*. Polytechnic International Press, Montreal, Quebec.
17. Kocurek, D. 1987. Lifting surface performance analysis for horizontal axis wind turbines. SERI/STR-2 17 3163. Solar Energy Research Insitute, Golden, CO.
18. Strickland, J. H., Smith, T., and Sun, K. 1981. A vortex model of the Darrieus turbine: an analytical and experimental study. SAND81-7017. Sandia National Laboratories, Albuquerque, NM.
19. Xu, G. and Sankar, L.N. 1999. Computational study of horizontal axis wind turbines. *A Collection of the 1999 ASME Wind Energy Symposium Technical Papers*, pp. 192–199.
20. Sørensen, N. N. and Hansen, M. O. L. 1998. Rotor performance predictions using a Navier–Stokes method. *A Collection of the 1998 ASME Wind Energy Symposium Technical Papers*, pp. 52–59.
21. Duque, E. P. N., Burkland, M. D., and Johnson, W. 2003. Navier–Stokes and comprehensive analysis performance predictions of the NREL phase VI experiment. *A Collection of the 2003 ASME Wind Energy Symposium Technical Papers*, pp. 43–61.
22. Sørensen, N., Michelsen, J., and Schreck, S. 2002. Navier-Stokes predictions of the NREL phase VI rotor in the NASA Ames 80 ft. x 120 ft. wind tunnel. *Wind Energy*, 5, 2/3, 151–169.
23. Johansen, J., Sørensen, N., Michelsen, J., Schreck, S. 2003. Detached-eddy simulation of flow around the NREL phase-VI rotor. *Proceedings of the 2003 European Wind Energy Conference and Exhibition*.
24. Xu, G. and Sankar, L. N. 2002. Application of a viscous flow methodology to the NREL phase VI rotor. *A Collection of the 2002 ASME Wind Energy Symposium Technical Papers*, pp. 83–89.
25. Simms, D., Schreck, S., Hand, M., and Fingersh, L. 2001. NREL unsteady aerodynamics experiment in the NASA-Ames wind tunnel: a comparison of predictions to measurements. NREL/TP-500-29494. National Renewable Energy Laboratory, Golden, CO.
26. ABAQUS Analysis User's Manual, Version 6.5. 2005. ABAQUS, Inc. Providence, Rhode Island, http://www.abaqus.com

27. MSC Adams, 2006. http://www.mscsoftware.com
28. Malcolm, D. J. and Wright, A. D. 1994. The use of ADAMS to model the AWT-26 prototype. *Proceedings of 1994 ASME Wind Energy Symposium*, pp. 125–132.
29. Molenaar, D. P. and Dijkstra, S. 1999. State-of-the-art of wind turbine design codes: main features overview for cost-effective generation. *Wind Engineering*, 23, 5, 295–311.
30. Buhl, M. L., Jr., Wright, A. D., and Pierce, K. G. 2000. Wind turbine design codes: a comparison of the structural response. *A Collection of the 2000 ASME Wind Energy Symposium Technical Papers*, pp. 12–22.
31. Quarton, D. C. 1998. The evolution of wind turbine design analyses—a twenty year progress review. *Wind Energy*, 1, 5–24.
32. RCAS Theory Manual, Version 2.0. 2002. United States (US) Army Aviation and Missile Command/AeroFlightDynamics Directorate (USAAMCOM/AFDD) Technical Report (TR). USAAMCOM/AFDD TR 02-A-005. US Army Aviation and Missile Command, Moffett Field, CA.
33. RCAS User's Manual, Version 2.0. 2002. United States (US) Army Aviation and Missile COMmand/AeroFlightDynamics Directorate (USAAMCOM/AFDD) Technical Report (TR). USAAMCOM/AFDD TR 02-A-006. US Army Aviation and Missile Command, Moffett Field, CA.
34. RCAS Applications Manual, Version 2.0. 2002. United States (US) Army Aviation and Missile COMmand/AeroFlightDynamics Directorate (USAAMCOM/AFDD) Technical Report (TR) TR 02-A-007. US Army Aviation and Missile Command, Moffett Field, CA.
35. Bir, G. S. and Chopra, I. 1994. University of Maryland Advanced Rotorcraft Code (UMARC) theory manual. Technical Report UM-AERO 94–18, Center for Rotorcraft Education and Research, University of Maryland, College Park, MD.
36. Lobitz, D. W. and Sullivan, W. N. 1983. A comparison of finite element prediction and experimental data for forced response of DOE 100 kW VAWT. *Proceedings of the Sixth Biennial Wind Energy Conference and Workshop*, pp. 843–853.
37. Mayda, E. A., van Dam, C. P., and Yen-Nakafuji, D. 2005. Computational investigation of finite width microtabs for aerodynamic load control. *A Collection of the 2005 ASME Wind Energy Symposium Technical Papers*, pp. 424–436.
38. Fuchs, E. F., Erickson, R. W., Carlin, P. W., and Fardou, A. A. 1992. Permanent magnet machines for operation with large speed variations. *Proceedings of the 1992 American Wind Energy Association Annual Conference*, American Wind Energy Association, Washington, DC, pp. 291–297.
39. Smith, G. A. 1989. Electrical control methods for wind turbines. *Wind Engineering*, 13, 88–98.
40. Manwell, J. F., McGowan, J. G., and Rogers, A. L. 2003. *Wind Energy Explained: Theory, Design and Application*. Wiley, Chichester.
41. Spera, D. ed. 1994. *Wind Turbine Technology, Fundamental Concepts of Wind Turbine Engineering*, ASME Press, New York.
42. Burton, T., Sharpe, D., Jenkins, N., and Bossanyi, E. 2001. *Wind Energy Handbook*. Wiley, Chichester.
43. Mandell, J. F. and Samborsky, D. D. 1997. DOE/MSU composite material fatigue database: test methods, materials, and analysis. SAND97-3002. Sandia National Laboratories, Albuquerque, NM.
44. Mandell, J. F., Samborsky, D. D., and Cairns, D. S. 2002. Fatigue of composite material and substructures for turbine blades. SAND2002-077. Sandia National Laboratories, Albuquerque, NM.
45. De Smet, B. J. and Bach, P. W. 1994. Database FACT: fatigue of composites for wind turbines. ECN-C-94-045. ECN, Petten, The Netherlands.
46. Kensche, C. W. ed. 1996. Fatigue of materials and components for wind turbine rotor blades. EUR 16684. European Commission, Luxembourg, Belgium.
47. Sutherland, H. J. 2000. A summary of the fatigue properties of wind turbine materials. *Wind Energy*, 3, 1, 1–34.

48. Griffin, D. A. 2004. Blade system design studies volume II: preliminary blade designs and recommended test matrix. SAND2004-0073. Sandia National Laboratories, Albuquerque, NM.
49. Jackson, K. J., Zuteck, M. D., van Dam, C. P., Standish, K. J., and Berry, D. 2005. Innovative design approaches for large wind turbine blades. *Wind Energy*, 8, 2, 141–171.
50. Krohn, S. 1997. *The energy balance of modern wind turbines. WindPower Note No. 16*. Danish Wind Turbine Manufacturers Association, Copenhagen.
51. Milborrow, D. 1998. Dispelling the myths of energy payback time. *Wind Stats Newsletter*, 11, 2, 1–3.
52. Malcolm, D. J. and Hansen, A. C. 2002. WindPACT turbine rotor design study: June 2000-June 2002. NREL/SR-500-32495. National Renewable Energy Laboratory, Golden, CO.
53. Sinclair, K. C. and Morrison, M. L. 1997. Overview of the U.S. Department of Energy/National Renewable Energy Laboratory avian research program. *Proceedings of Windpower '97*, American Wind Energy Association, Washington, DC, pp. 273–279.
54. Sinclair, K. C. 1999. Status of the U.S. Department of Energy/National Renewable Energy Laboratory avian research program. *Proceedings of Windpower '99*, American Wind Energy Association, Washington, DC, pp. 273–279.
55. Colson, E. W. 1995. Avian interactions with wind energy facilities: a summary. *Proceedings of Windpower '95*, American Wind Energy Association, Washington, DC, pp. 77–86.
56. Wolf, B. 1995. Mitigating avian impacts: applying the wetlands experience to wind farms. *Proceedings of Windpower '95*, American Wind Energy Association, Washington, DC, pp. 109–116.
57. Erickson, W. P., Johnson, G. D., Strickland, M. D., Young, D. P., Sernka, K. J., and Good, R. E. 2001. Avian collisions with wind turbines: a summary of existing studies and comparisons to other sources of avian collision mortality in the United States. National Wind Coordinating Committee, Washington, DC http://www.nationalwind.org/publications/wildlife/avian_collisions.pdf.

Further Information

Excellent summaries of HAWT and VAWT aerodynamics, together with extensive reference lists, are presented by Hansen and Butterfield [12], and by Touryan, Strickland, and Berg [15], respectively. Volume 1, number 1 of *Wind Energy*, Wiley, 1998 contains a comprehensive set of review papers covering wind turbine rotor aerodynamics, design analysis, and overall system design.The latest developments in the field of wind energy in the United States and Europe may be found in the following annual conference proceedings: *A Collection of the ASME Wind Energy Symposium Technical Papers*, American Institute of Aeronautics and Astronautics, 59 John Street, 7th Floor, New York, NY 10038. *Proceedings of Windpower*, American Wind Energy Association (AWEA), 1101 14th St. NW, 12th Floor, Washington, DC 20005. *Proceedings of the European Wind Energy Association*, European Wind Energy Association, Renewable Energy House, Rue d'Arlon 63-65, BE-1040 Brussels. Belgium. *Proceedings of the British Wind Energy Association*, British Wind Energy Association, Renewable Energy House, 1 Aztec Row, Berners Road, London, N1 0PW, UK. The books by Manwell, et al. [40], Spera [41] and Burton et al. [42] contain a wealth of fairly current information on wind energy conversion, history, and technology, together with extensive reference lists. The National Wind Coordinating Committee [57] gives a good account of the studies that have been done of wind turbine/bird collisions and puts the results in context with bird deaths due to other causes. Extensive information on wind energy conversion technology may also be found on the World Wide Web. Excellent sites to start with include those of the U.S. National Renewable Energy Laboratory Wind Energy Technology Center at http://www.nwtc.nrel.gov, Sandia National Laboratories Wind Energy Technology Department at http://www.sandia.gov/wind, the Danish Risø National Laboratory at http://www.risoe.dk/vea/index.htm, the American Wind Energy Association at http://www.awea.org, the British Wind Energy Association at http://www.britishwindenergy.co.uk, the European Wind Energy Association at http://www.ewea.org, and the Danish Wind Industry Association at http://www.windpower.org/en/core.htm.